PAPER Nr. : 17

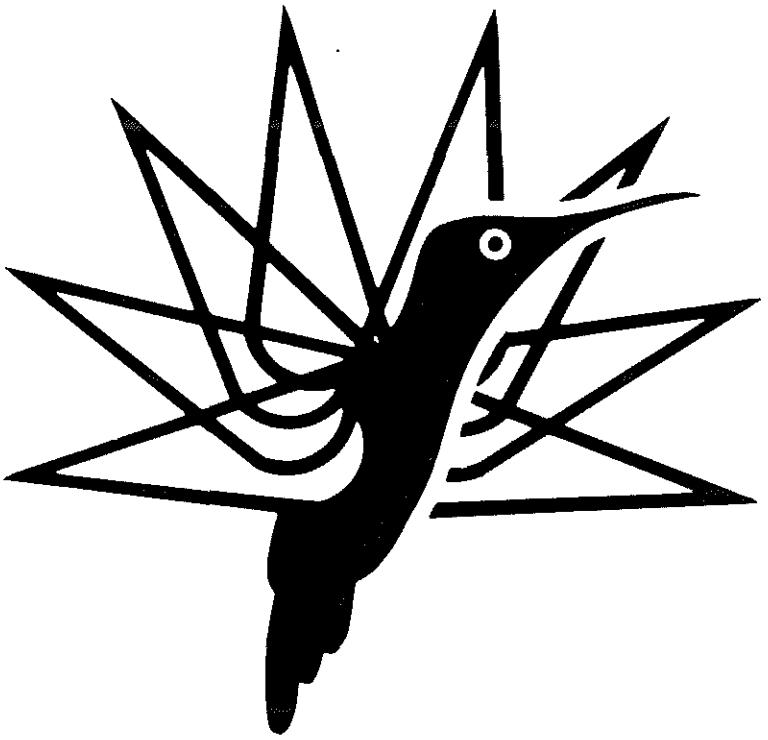

GLAUERT AUGMENTATION OF ROTOR INFLOW DYNAMICS

R. Bradley+

C.G. Black+

D.J. Murray-Smith*

Department of Aerospace Engineering+

and

Department of Electronics and Electrical Engineering*
University of Glasgow,
Glasgow, G12 8QQ, U.K.

FIFTEENTH EUROPEAN ROTORCRAFT FORUM

SEPTEMBER 12 - 15, 1989 AMSTERDAM

GLAUERT AUGMENTATION OF ROTOR INFLOW DYNAMICS

R. Bradley, C.G. Black, D.J. Murray-Smith

University of Glasgow

ABSTRACT

The demands of modern agile rotorcraft necessitate the use of high-bandwidth control and actuation systems. The models currently used for simulation and flight control system design must therefore be extended to cover the range of frequencies which encompass the rotor dynamics, including the dynamics of induced flow. The basic models of inflow using local momentum theory and simple vortices have been examined over a range of frequencies using parameter identification techniques and have been found to be inadequate. This paper presents a model incorporating a Glauert type of augmentation and uses flight data to justify its validity.

NOMENCLATURE

A	System matrix of rotor
B	Effective control matrix for state-space representations
C	Coefficient matrix of $\underline{\beta}'$ in flapping equation
D	Coefficient matrix of $\underline{\beta}$ in flapping equation
E	Coefficient matrix of $\underline{x}'$ in modified state equation
H	Measurement matrix
D_τ, D_τ^*	Diagonal matrices of induced-flow time constants
H_λ	Coefficient matrix for $\underline{\lambda}$ in flapping equation
H_θ	Coefficient matrix for $\underline{\theta}$ in flapping equation
H_η	Coefficient matrix for $\underline{\eta}$ in flapping equation
F_β	Coefficient matrix for $\underline{\beta}$ in non-dimensional dynamic induced-flow equation
$F_{\beta'}$	Coefficient matrix for $\underline{\beta}'$ in non-dimensional dynamic induced-flow equation
F_θ	Coefficient matrix for $\underline{\theta}$ in non-dimensional dynamic induced-flow equation
F_η	Coefficient matrix for $\underline{\eta}$ in non-dimensional dynamic induced-flow equation
F_ν	Coefficient matrix for $\underline{\nu}$ in non-dimensional dynamic

	induced flow equation
$\underline{x}$	State vector
$\underline{u}$	Control vector
$\underline{\beta}$	Vector of harmonic components of blade flap
$\underline{\theta}$	Vector of harmonic components of blade pitch
$\underline{\lambda}$	Vector of harmonic components of non-dimensional induced-flow
$\underline{\eta}$	Vector of non-dimensional pitch and roll accelerations
$\underline{\nu}$	Vector of non-dimensional inflow due to hub motion
τ	Non-dimensional induced flow time constant
τ_0	Non-dimensional time constant associated with λ_0 dynamics
τ_{cs}	Non-dimensional time constant associated with λ_c and λ_s dynamics
$\underline{z}$	Measurement vector
$\underline{v}$	Measurement noise vector
J	Cost function
$\underline{\epsilon}$	Vector of residuals (frequency domain)
Ω	Angular rotor speed
R	Blade radius
ψ	Blade azimuth angle
$\bar{r}$	Normalised radial blade position
V	Resultant air speed through rotor disc
$\underline{c}$	Aerodynamic force and moment vector
L	Aerodynamic coefficient matrix
μ_x, μ_y	Non-dimensional longitudinal and lateral components of rotor hub velocity
μ	Non-dimensional velocity in the plane of the rotor disc ($\mu^2 = \mu_x^2 + \mu_y^2$)
μ_z	Non-dimensional component of rotor hub velocity normal to the rotor plane
$\bar{w}_B$	Non-dimensional component of blade velocity normal to the blade
n_β	Inertia number
λ_β	Normalised flapping frequency
K	Matrix of Glauert-type constants for empirical model
k_{ij}	Glauert-type constants for extended theoretical model
$c_i, \bar{c}_i$	Glauert-type constants and corresponding mean values for extended theoretical model

1. INTRODUCTION

The demands of the modern agile helicopter and other rotorcraft necessitate high bandwidth control and actuation systems. Mathematical models currently in use for real-time simulations and for flight control system design must therefore be extended to cover the range of frequencies which encompass the rotor dynamics, including the dynamics of induced flow. The dynamic modelling of induced flow in helicopter rotors is therefore a topic which is currently receiving much attention.[1,2]

System identification methods provide the basis of one approach to the development and validation of improved rotor models and previous work carried out at the University of Glasgow has provided a general methodology based upon these techniques[3-6]. Many models for induced flow effects have been suggested and the parameter identification

approach has been applied both to models based on local momentum theory and to models based on vortex theory[1]. Within this identification-based approach the ability of the model to represent the important features of the real system is assessed not only in terms of the goodness of fit between responses predicted by the model and the equivalent measured responses from flight data but also from the estimated confidence levels associated with parameter values and the credibility of estimates in physical terms.

The development of a practical model of induced flow through the rotor for application to real time helicopter simulation has to balance the need for fidelity with the exigencies of a real time environment. The compromise in complexity which this balance requires is often best approached by taking a basic simplistic model and subsequently introducing a phased enhancement until the point is reached where acceptable predictions are achieved. The preferred approach to model building is that based on physical principles rather than one which is directly heuristic, since an economy of parameters often results, and these parameters are usually physically meaningful quantities where a priori estimates are available. Further, the physical approach inherently incorporates simplifications which can point the way to later enhancements

2. FIRST-ORDER BLADE-FLAPPING MODEL WITH BASIC INDUCED-FLOW DYNAMICS

Although the most general form of model for blade flapping considered in the previous work involved retaining the second derivatives of the flapping components, it has been found that it is justifiable to neglect them to reduce the model to a first-order system that includes the dynamics of the induced flow[1]. The resulting equations have the following form:

$$\begin{bmatrix} C & 0 \\ -F_{\beta'} & D_\tau \end{bmatrix} \begin{bmatrix} \underline{\beta} \\ \underline{\lambda} \end{bmatrix}' = \begin{bmatrix} -D & H_\lambda \\ F_\beta & (F_\lambda - I) \end{bmatrix} \begin{bmatrix} \underline{\beta} \\ \underline{\lambda} \end{bmatrix} + \begin{bmatrix} H_\theta & H_\nu & H_\eta \\ F_\theta & F_\nu & 0 \end{bmatrix} \begin{bmatrix} \underline{\theta} \\ \underline{\nu} \\ \underline{\eta} \end{bmatrix} \quad (1)$$

where

$\underline{\beta} = (\beta_0, \beta_{1c}, \beta_{1s})^T$ are the flapping components of the multiblade representation.

$\underline{\theta} = (\theta_0, \theta_{1cw}, \theta_{1sw})^T$ are collective, lateral and longitudinal components of the blade pitch respectively in hub wind axes[2].

$\underline{\nu} = (\mu_z, \bar{q}_w, \bar{p}_w)^T$ are the non-dimensional quantities: component of rotor hub velocity normal to the rotor plane, pitch and roll rates of the rotor in hub wind axes.[2]

$\underline{\lambda} = (\lambda_0, \lambda_{1c}, \lambda_{1s})^T$ are the mean and harmonic components of the induced flow.

$\underline{\eta} = (q'_w, p'_w)^T$ are the non-dimensional pitch and roll accelerations.

The matrices appearing in equation 1 have elements which depend upon the fundamental parameters λ_β, the normalised flapping frequency, and n_β the inertia number as follows:

$$C = \begin{bmatrix} n_\beta & 0 & \frac{2}{3}\mu n_\beta \\ 0 & n_\beta & 2 \\ \frac{4}{3}\mu n_\beta & -2 & n_\beta \end{bmatrix} \quad D = \begin{bmatrix} \lambda_\beta^2 & 0 & 0 \\ \frac{4}{3}\mu n_\beta & \lambda_\beta^2 - 1 & n_\beta\left[1+\frac{\mu^2}{2}\right] \\ 0 & -n_\beta\left[1-\frac{\mu^2}{2}\right] & \lambda_\beta^2 - 1 \end{bmatrix}$$

$$H_\theta = \begin{bmatrix} n_\beta\left[1+\mu^2\right] & 0 & \frac{4}{3}\mu n_\beta \\ 0 & n_\beta\left[1+\frac{\mu^2}{2}\right] & 0 \\ \frac{8}{3}\mu n_\beta & 0 & n_\beta\left[1+3\mu^2\right] \end{bmatrix} \quad H_\eta = \begin{bmatrix} 0 & 0 \\ 1 & 0 \\ 0 & 1 \end{bmatrix}$$

$$H_\nu = \begin{bmatrix} \frac{4}{3} n_\beta & 0 & \frac{2}{3}\mu n_\beta \\ 0 & n_\beta & 2 \\ 2\mu n_\beta & -2 & n_\beta \end{bmatrix}$$

$$H_\lambda = \begin{bmatrix} -\frac{4}{3} n_\beta & 0 & -\frac{2}{3}\mu n_\beta \\ 0 & -n_\beta & 0 \\ -2\mu n_\beta & 0 & -n_\beta \end{bmatrix}$$

The non-dimensional component of hub velocity in the plane of the rotor, μ, also appears within these matrices, but in the absence of perturbations in μ the equation is linear and may be used for cases involving perturbations in $\underline{\beta}$, $\underline{\theta}$, $\underline{\nu}$, $\underline{\lambda}$ and $\underline{\eta}$.

2.1 The Basic Induced-Flow Model

The dynamic model for the induced flow takes the general form:

$$\tau\, \underline{\lambda}' + \underline{\lambda} = L\, \underline{c} \qquad (2)$$

where the forcing term involves a non-dimensional aerodynamic force and moment vector

$$\underline{c} = (C_T/a_o s,\ C_{mc}/a_o s,\ C_{ms}/a_o s)^T \qquad (3)$$

The quantity C_T is the normalised rotor thrust while C_{mc} and C_{ms} are the normalised moments about the rotor y and x axes respectively. The quantities s and a_o are the rotor solidity and the blade lift slope.

The aerodynamic force and moments can be related to variables used in the model defined by equation 1 in the following way[1]:-

$$\underline{c} = G_{\beta'}\underline{\beta'} + G_{\beta}\underline{\beta} + G_{\theta}\underline{\theta} + G_{\nu}\underline{\nu} + G_{\lambda}\underline{\lambda} \qquad (4)$$

Here the matrices $G_{\beta'}$, G_{β}, G_{θ}, G_{ν} and G_{λ} all involve elements which are functions of μ, the non-dimensional speed in the plane of the rotor disc[1]. For the purposes of the work described the value of μ was assumed constant and was obtained from the flight data used in the system identification.

The form of the matrix L is determined by the type of model adopted and one widely used form is derived from local momentum theory [7]. By considering the force, dF, on an element of the rotor disc and by integrating this over the rotor-disc area with appropriate weightings it is possible to derive expressions for the rotor thrust and moments. These are the elements of the $\underline{c}$ vector as defined in equation 3. In the case of the thrust, for example, this can be show to give

$$T = \int_s dF = \int_0^{2\pi}\int_0^R 2\rho v_i V r dr d\psi \qquad (5)$$

where v_i is the induced velocity through the rotor disc and V is the resultant speed of air through the disc.

Different forms can be assumed for the induced velocity. The form chosen for the present work involves a radial variation[2,8] as follows:-

$$\lambda_i = \frac{v_i}{\Omega R} = \lambda_o + \lambda_{1c}\bar{r}\cos\psi + \lambda_{1s}\bar{r}\sin\psi \qquad (6)$$

The resulting speed of air through the disc can be written in the form:

$$\frac{V}{\Omega R} = (\mu^2 + (\mu_z - \lambda_i)^2)^{1/2} \qquad (7)$$

where μ_z is the component of aerodynamic velocity of the rotor hub (non-dimensional) normal to the rotor plane. The factor ΩR which appears in both equations 6 and 7 is introduced for purposes of normalisation.

In previous work carried out at the University of Glasgow[1] the quantity $V/\Omega R$ was approximated by μ for fast forward flight. From integrals similar to that in equation 5 it was possible to derive a basic inflow equation in which the matrix L was of diagonal form with constant coefficients. Substitution of equation 4 into equation 2 allowed the induced-flow model to be incorporated into the first-order blade flapping model and thus gave the combined form of model given by equation 1.

2.2 The System Identification Method

Equation 1 may be manipulated without difficulty into the standard state-space form. However, to facilitate the direct estimation of physical parameters, such as λ_β and n_β, there are advantages in retaining the general form:

$$E\underline{x}' = A\underline{x} + B\underline{u} \qquad (8)$$

For the model structure of equation 1 it is possible to express equation 8 in partitioned form as follows:-

$$\begin{bmatrix} E_{11} & 0 \\ E_{21} & E_{22} \end{bmatrix} \begin{bmatrix} \underline{\beta} \\ \underline{\lambda} \end{bmatrix}' = \begin{bmatrix} A_{11} & A_{12} \\ A_{21} & A_{22} \end{bmatrix} \begin{bmatrix} \underline{\beta} \\ \underline{\lambda} \end{bmatrix} + \begin{bmatrix} B_{11} & B_{12} & B_{13} \\ B_{21} & B_{22} & 0 \end{bmatrix} \begin{bmatrix} \underline{\theta} \\ \underline{\nu} \\ \underline{\eta} \end{bmatrix} \qquad (9)$$

This equation retains the structural features of the theoretical model described by equation 1 and provides a basis for the application of system identification and parameter estimation techniques.

Estimation of parameters within the model given by equation 9 may be carried out conveniently in the frequency domain using an output–error approach. In the frequency domain equation 8 has the form:

$$E\ \underline{X}'(\omega) \;=\; A\ \underline{X}(\omega) \;+\; B\ \underline{U}(\omega) \qquad (10)$$

The measured quantities, $\underline{Z}(\omega)$, are then related to the state variables $\underline{X}(\omega)$ through the equation

$$\underline{Z}(\omega) \;=\; H\ \underline{X}(\omega) \;+\; \underline{V}(\omega) \qquad (11)$$

where $\underline{V}(\omega)$ is assumed to be band–limited white noise. Unbiased model parameters are obtained using output–error methods provided that there is negligible process noise and that the measurement noise band limit lies beyond the frequency range used in the identification.

The cost function which is minimised in the frequency–domain output–error approach takes the form

$$J \;=\; \sum_{\omega_1}^{\omega_2} \left[\ \underline{\epsilon}^{*}\ S^{-1}\ \underline{\epsilon} \;+\; \log_e\ |S|\ \right] \qquad (12)$$

where $\underline{\epsilon}$ represents the difference between the observations and the model output in the frequency domain. S is the error–covariance matrix defining the noise statistics of the measured responses Z and $[\omega_1,\ \omega_2]$ represents the range of frequencies used in the identification.

For the case being considered the measured quantities are elements of the state vector $\underline{x} = (\underline{\beta}, \underline{\lambda})^T$ and thus the measurement transition matrix, H, is the identity matrix. Measurements of $\underline{\beta}$ are available and the elements of the error–covariance matrix S in equation 12 associated with this vector are also estimated as part of the identification process. Measurements of the induced flow states $\underline{\lambda}$ are not available and the approach adopted involves fixing the corresponding elements of S at very large (effectively infinite) values. This indicates the uncertainty in the non–existent measured responses for $\underline{\lambda}$ and enables the identification to proceed.

Important features of the frequency–domain method for rotorcraft system identification which has been developed at the University of Glasgow[3] include the ease with which the frequency range used for the identification can be controlled, the ability to estimate time shifts in the input and output vectors and a facility for defining relationships between different elements within the model structure. In the model given by equation 1 the matrix elements are functions of a few parameters and it is generally a sound principle to take full account of known relationships between elements of the matrices. The estimation of $^{n}_{\beta}$ and λ^2_{β} is of particular interest in the current work and the ability to define relationships between parameters is therefore a particularly valuable feature of the identification method.

2.3 Identification Results for the Basic Induced–Flow Model

Results obtained from the use of the momentum–inflow model of equation 1 showed that although satisfactory fits could be obtained for β_o and β_{1c} the correspondence between the measured and predicted responses for β_{1s} was relatively poor[1]. This deficiency in the previously published results was particularly marked in terms of comparisons in the frequency domain which indicated significant differences, especially in terms of phase. These earlier results are reproduced in Figure 1 with the corresponding estimates of parameters being shown in Table 1. The results show that a high value of normalised blade flapping frequency, λ_{β}, was obtained, compared with theory. It can also

be seen that the single time constant τ, associated with the induced-flow dynamics, was estimated with considerable uncertainty. The flight test data used in this work were obtained from a Puma helicopter flying at 100 knots with a rotor speed of 27.5 rad/s. A longitudinal-cyclic doublet input was applied by the pilot during the run. The frequency range used in the identification was 0.226 Hz to 1.60 Hz.

As a first step in seeking an improved model, the longitudinal and lateral components of hub velocity, μ_x and μ_y respectively, were introduced within the induced-flow model. Such terms are included in other inflow models[9] and their introduction, on a purely empirical basis, led to a new model for the induced-flow dynamics having the following form:-

$$D^*_\tau \underline{\lambda}' + \underline{\lambda} = L\underline{c} + K\mu_{xy} \qquad (13)$$

where

$$K = \begin{bmatrix} k_{01} & k_{02} \\ k_{11} & k_{12} \\ k_{21} & k_{22} \end{bmatrix} \qquad \mu_{xy} = (\mu_x, \mu_y)^T$$

In this equation D^*_τ is a diagonal matrix involving two independent time constants: a time constant τ_o associated with the λ_o dynamics and a second time constant τ_{cs} associated with both λ_{1c} and λ_{1s}.

$$D^*_\tau = \begin{bmatrix} \tau_o & 0 & 0 \\ 0 & \tau_{cs} & 0 \\ 0 & 0 & \tau_{cs} \end{bmatrix}$$

The matrix D_τ in equation 1 involves three equal time constants.

The identification based upon the empirical model of equation 13 was performed using the same flight data and the same frequency range (0.226 Hz - 1.60 Hz) as for the

basic model. The identification included estimation of a bias term in the recorded blade azimuth position. This was estimated as a shift (in radians) in the measured responses for multiblade flapping, $\underline{\beta}$, and pitch, $\underline{\theta}$. The estimation process for these measurement system parameters made use of the facility within the identification software for estimation of time shifts and also of the facility for defining relationships between elements of a model. Through the use of this latter facility a single value of bias was estimated which represented a parameter occurring at six points within the model.

Results obtained from application of the system identification approach to the empirical model of equation 13 are given in Table 2. The corresponding frequency-domain fits and time-domain reconstructions are shown in Figure 2 and Figure 3 respectively. It can be seen that the changes in the model have resulted in substantially improved fits. In addition, the normalised flapping frequency, λ_β, is now in much better agreement with theory than for the previous case given in Table 1. The inertia number, n_β is still in good agreement with theory and many of the empirical constants, k_{ij}, are estimated with relatively low error bounds. The two induced-flow time constants, τ_0 and τ_{cs}, are found to have values which are rather larger than might have been expected from physical considerations, especially in the case of τ_0 which is the time constant associated with λ_0 dynamics. An azimuth bias term, which has been used to advantage by others[9], is estimated with a low error bound and corresponds to a bias of about 16.2 degrees.

3. A MODIFIED FIRST-ORDER BLADE-FLAPPING MODEL WITH INDUCED-FLOW DYNAMICS

The favourable results obtained using the empirical model of equation 13 suggested that an improved theoretical model structure should be sought. It was believed that an a model could allow a physical interpretation to be placed upon the estimates of the empirical parameters within the K matrix defined in equation 13.

3.1 An Extended Induced-Flow Model

One problem area associated with the basic model of induced flow concerns the equation defining the speed of air through the disc (equation 7). If μ_z, the component of rotor hub velocity normal to the rotor plane, is replaced by $\bar{W}_B$, the blade velocity in non-dimensional form, we have

$$\frac{V}{\Omega R} = (\mu^2 + (\bar{W}_B - \lambda_i)^2)^{1/2} \qquad (14)$$

where

$$\bar{W}_B = \mu_z + [\bar{r}p^* + T_1]\sin\psi + [\bar{r}q^* + T_2]\cos\psi + \tfrac{1}{2}\theta^*_o \qquad (15)$$

where

$$p^* = p/\Omega + \beta_{1c} - \beta'_{1s} + \theta_{1s}$$

$$q^* = q/\Omega - \beta_{1s} - \beta'_{1c} + \theta_{1c}$$

$$T_1 = \beta_o\mu_y + \theta_o\mu_x$$

$$T_2 = -\beta_o\mu_x + \theta_o\mu_y$$

$$\theta^*_o = 2\bar{r}\theta_o + \mu_x\theta_{1s} + \mu_y\theta_{1c} - \mu_x\beta_{1c} + \mu_y\beta_{1s}$$

In this equation it should be noted that the derivatives β'_{1s} and β'_{1c} involve differentiation with respect to azimuth (normalised time).

From equations 14 and 15 the following approximate expression can be derived

$$(\mu^2 + (\bar{W}_B - \lambda_i)^2)^{\frac{1}{2}} \simeq \mu + \frac{\bar{\lambda}_o}{\mu}\left[(\bar{r}(p^* - \lambda_{1s}) + T_1)\sin\psi + (\bar{r}(q^* - \lambda_{1c}) + T_2)\cos\psi\right] \qquad (16)$$

where $\bar{\lambda}_o$ represents a mean value of λ^*_o where

$$\lambda_o^* = \mu_z - \lambda_o + \tfrac{1}{2}\theta_o^* \qquad (17)$$

Using equations 6 and 16 we have:

$$v_i V \simeq \Omega^2 R^2(\lambda_o + \lambda_{1c}\bar{r}\cos\psi + \lambda_{1s}\bar{r}\sin\psi)\ (\mu + \frac{\bar{\lambda}_o}{\mu}\left[(\bar{r}(p^* - \lambda_{1s}) + T_1)\sin\psi\right.$$

$$\left. + (\bar{r}(q^* - \lambda_{1c}) + T_2)\cos\psi\right]) \qquad (18)$$

The expression given in equation 18 can then be used within integrals similar to that in equation 5 in order to calculate expressions for the aerodynamic forces and moments. This leads to the following modified form of induced flow equation:-

$$D_\tau^* \underline{\lambda}' + \underline{\lambda} = L\underline{c} + F\underline{\nu}_\lambda + G\underline{\mu}_{xy} \qquad (19)$$

where

$$L = \begin{bmatrix} a_o s/2\mu & 0 & 0 \\ 0 & -2a_o s/\mu & 0 \\ 0 & 0 & -2a_o s/\mu \end{bmatrix}$$

$$F = \begin{bmatrix} \bar{k}_s & \bar{k}_c \\ 0 & \bar{k}_o \\ \bar{k}_o & 0 \end{bmatrix} \qquad G = \begin{bmatrix} \bar{c}_1 & \bar{c}_2 \\ -\bar{c}_3 & \bar{c}_4 \\ \bar{c}_4 & \bar{c}_3 \end{bmatrix}$$

$$\underline{\nu}_\lambda = (p^* - \lambda_{1s},\ q^* - \lambda_{1c})^T$$

$$\underline{\mu}_{xy} = (\mu_x,\ \mu_y)^T$$

and where $\bar{k}_s$, $\bar{k}_c$ and $\bar{k}_o$ and $\bar{c}_1$, $\bar{c}_2$, $\bar{c}_3$ and $\bar{c}_4$ are constants representing the mean values of the following quantities:

$$k_s = \frac{-\lambda_{1s}\bar{\lambda}_o}{4\mu^2\Omega} \qquad k_c = \frac{-\lambda_{1c}\bar{\lambda}_o}{4\mu^2\Omega} \qquad k_o = \frac{-\lambda_o\bar{\lambda}_o}{2\mu^2\Omega}$$

$$c_1 = \frac{4}{3} k_s \Omega\theta_o - \frac{4}{3} k_c \Omega\beta_o$$

$$c_2 = \frac{4}{3} k_s \Omega\beta_o + \frac{4}{3} k_c \Omega\theta_o$$

$$c_3 = \frac{8}{3} k_o \Omega\beta_o$$

$$c_4 = \frac{8}{3} k_o \Omega\theta_o$$

The matrix G represents a Glauert type of augmentation to the induced flow model.

3.2 The Blade-Flapping Model with Extended Induced-Flow Dynamics

The incorporation of the extended induced-flow model of equation 19 into the state-space description for flap and induced velocity given originally by equation 1 requires some changes. Firstly there is a requirement to introduce the quantities μ_x and μ_y as measured inputs. This implies a need to estimate elements of the associated coefficient matrix G. Secondly, the term $F\underline{\nu}_\lambda$ in equation 19 involves terms from the vectors $\underline{\beta}'$, $\underline{\beta}$. $\underline{\lambda}$, $\underline{\theta}$ and $\underline{\nu}$ and thus modifies the definitions of the partition matrices E_{21}, A_{21}, A_{22}, B_{21} and B_{22} of equation 9. Additional constants associated with k_s, k_c and k_o must also be estimated. The complete model now has the form:

$$\begin{bmatrix} E_{11} & 0 \\ E^*_{21} & E^*_{22} \end{bmatrix} \begin{bmatrix} \underset{\sim}{\beta} \\ \underset{\sim}{\lambda} \end{bmatrix}' = \begin{bmatrix} A_{11} & A_{12} \\ A^*_{21} & A^*_{22} \end{bmatrix} \begin{bmatrix} \underline{\beta} \\ \underline{\lambda} \end{bmatrix}$$

$$+ \begin{bmatrix} B_{11} & B_{12} & B_{13} & 0 \\ B^*_{21} & B^*_{22} & 0 & G \end{bmatrix} \begin{bmatrix} \underline{\theta} \\ \underline{\nu} \\ \underline{\eta} \\ \mu_{xy} \end{bmatrix} \quad (20)$$

3.3 Parameter Identification using the Modified Model

Examination of equation 19 shows that the more complex model structure resulting from the introduction of Glauert augmentation involves a number of constants which are

interrelated. However, by further manipulation of the relationships given above, it can be shown that the quantities $\bar{k}_c$, $\bar{k}_s$ and $\bar{k}_o + a_o s/8\mu$ may be estimated as independent parameters.

The application of parameter estimation techniques for this new model structure with the flight test data used previously led to the results presented in Table 3 and in Figures 4 and 5. From Table 3 it can bee seen that the estimates of the physical parameters λ^2_β and n_β are identical, within the indicated error bounds, to those obtained for the empirical model as presented in Table 2. However, the estimates obtained for the time constants given in Table 3 are substantially different from those in Table 2. The time constants obtained for the modified model structure indicate that the λ_o dynamics are almost instantaneous and that the λ_{1c} and λ_{1s} dynamics have a time constant of about 0.8 seconds. The time constant τ_{cs} is estimated with a high degree of confidence and from a physical standpoint these values are much more satisfactory than those for the empirical model. The quantities $\bar{k}_c$ and $\bar{k}_s$ introduced in Section 3.1 have estimated error bounds which indicate a reasonable degree of confidence while the error bound for the paramter $\bar{k}_o$ indicates complete uncertainty in terms of the estimate. The coefficients $\bar{c}_1$, $\bar{c}_2$, $\bar{c}_3$ and $\bar{c}_4$ associated with the μ_x and μ_y inputs to the induced-flow equation show values close to zero for those corresonding to λ_o (i.e. $\bar{c}_1$ and $\bar{c}_2$) and are estimated with a very high degree of confidence for those corresponding to λ_{1c} and λ_{1s} (i.e. $\bar{c}_3$ and $\bar{c}_4$). This means that two independent parameters, $\bar{c}_3$ and $\bar{c}_4$, together with the relationships indicated by equation 19, are now estimated in place of the four independent parameters k_{11}, k_{12}, k_{21} and k_{22} in the empirical model structure.

Comparing Figure 4 with Figure 2 it can be seen that very similar fits better fits are obtained for β_o and β_{1c} with the modified and empirical model structures. In the case of β_{1s} the results for the empirical model, as presented in Figure 2, show a better magnitude comparison, at the important lower frequencies. It should be noted, however, that the magnitude of β_{1s} is very small in comparison with β_{1c}.

3.4 Effect of Frequency Range on Parameter Estimates

The effect on the estimated values of varying the lowest frequency used in the identification is shown in Figure 6. The range of starting frequencies considered covered the lowest available frequency of 0.0376 Hz up to a value of 0.338 Hz which excludes the rigid-body dynamics.

If we exclude consideration of the lowest available frequency (0.0376 Hz) and consider initial frequency values in the range 0.0752 Hz to 0.2256 Hz it can be seen that many of the parameter estimates are effectively independent of frequency range. Such parameters include the inertia number n_β, the induced-flow time constants τ_o and τ_{cs}, the normalised flapping frequency λ_β^2, the induced-flow model coefficients for both μ_x and μ_y, $\bar{c}_1$ and $\bar{c}_4$, and the azimuth bias. There is some variation with frequency for the estimate of k_s, and in the cases of k_c and $(k_o + a_o s/8\mu)$ there is a considerable variation. These terms do, however, depend on time-varying quantities and some variation with frequency range might be expected.

4. CONCLUSIONS

A frequency-domain output-error system identification technique has been applied successfully to the estimation of parameters of a state-space type of model representing rotor flapping and induced velocity for a Puma helicopter. Many features of the particular frequency-domain approach used and its software implementation were found to be specially appropriate for this form of modelling problem.

The development of the model structure used in the identification involved extension of an earlier momentum-inflow model by means of empirical modifications which were subsequently justufied by additional theoretical work. In essence, these changes amounted to a more complex representation of the rotor surface used in the momentum-inflow theory, incorporating effects due to blade flap and blade pitch.

The identification software used for this work accommodated the changes in model structure without difficulty. The facility within this software for incorporating defined relationships between different elements of the model structure was found to be an essential tool for this work.

The fundamental physical parameters in the extended model structure (i.e. λ_β^2 , n_β, τ_o and τ_{cs}) were confidently estimated with values that were physically realistic and fairly constant for a range of frequencies. The introduction of two distinct time constants associated with the induced-flow dynamics (τ_o and τ_{cs}) was found to be a valid modelling step. An effectively instantaneous response was found for the λ_o dynamics and a time constant of the order of 0.8 seconds was estimated with small error bounds for both the λ_{1c} and λ_{1s} dynamics.

The model structure developed ultimately in this paper for blade flap and induced velocity exemplifies how through the use of sound physical reasoning and versatile software tools, adequate mathematical models incorporating observed physical features can be developed by means of system identification methods.

5. ACKNOWLEDGEMENTS

The authors would like to acknowledge the contribution of Dr. G.D. Padfield of the Royal Aerospace Establishment, Bedford, to this work. The research was carried out as part of the Ministry of Defence Extramural Agreement 2048/46/XR/STR.

6. REFERENCES

1. R. Bradley, C.G. Black, D.J. Murray-Smith; "System Identification Strategies for Helicopter Rotor Models Incorporating Induced Flow". Vertica, Vol. 13, No. 3, 281-294, 1989.

2. G.D. Padfield; "A Theoretical Model of Helicopter Flight Mechanics for Application to Piloted Simulation", RAE TR 81048, April 1981.

3. C.G. Black; "A Methodology for the Identification of Helicopter Mathematical Models from Flight Data Based on the Frequency Domain", Ph.D. Thesis, Department of Aerospace Engineering, University of Glasgow, July 1988.

4. C.G. Black; "A User's Guide to the System Identification Programs OUTMOD and OFBIT, Department of Aerospace Engineering/Department of Electronics and Electrical Engineering Internal Report, February, 1989.

5. C.G. Black, D.J. Murray-Smith, G.D. Padfield, "Experience with Frequency-Domain Methods in Helicopter System Identification", 12th European Rotorcraft Forum, Garmisch-Partenkirchen, Federal Republic of Germany, September 1986, Paper 76.

6. C.G. Black, "Consideration of Trends in Stability and Control Derivatives from Helicopter System Identification", 13th European Rotorcraft Forum Arles, France, September 1987, Paper 7.8.

7. R.A. Ormiston, D.A. Peters, "Hingeless Helicopter Rotor Response with Non-uniform Inflow and Elastic Blade Bending", J. Aircraft, Vol. 9, No. 10, 1972.

8. W. Johnson, "Helicopter Theory", Princetown University Press, 1980.

9. R.W. DuVal, O.Bruhis, J.A. Green, "Derivation of a Coupled Flapping/Inflow Model for the Puma Helicopter". Vertica, Vol. 13, No. 3, 267-280, 1989.

TABLE 1 Physical parameter estimates for original model structure

PARAMETER	ESTIMATE (0.226 – 1.58 Hz)	APPROXIMATE THEORETICAL VALUE
$1 - \lambda_\beta^2$	−0.3992 (0.084)†	
λ_β^2	1.3992	1.06
n_β	1.0027 (0.11)†	0.987
τ	19.426 (11.0)†	–

† Estimated 1 σ error bound.

TABLE 2 Parameter estimates for empirical model

PARAMETER	ESTIMATE (0.226 – 1.58 Hz)	APPROXIMATE THEORETICAL VALUE
$1 - \lambda_\beta^2$	−0.0703 (0.025)†	
λ_β^2	1.07	1.06
n_β	0.906 (0.035)†	0.987
τ_o	16.28 (5.107)†	–
τ_{cs}	31.91 (2.23)†	–
k_{01}	−0.279 (0.12)†	–
k_{02}	0.0583 (0.008)†	–
k_{11}	−1.105 (0.36)†	–
k_{12}	−1.835 (0.12)†	–
k_{21}	−0.168 (0.14)†	–
k_{22}	−0.698 (0.058)†	–
ψ_{BIAS}	0.283 (0.042)†	–

† Estimated 1 σ bound.

TABLE 3 Parameter estimates for improved model structure

PARAMETER	ESTIMATE (0.226 - 1.58 Hz)	APPROXIMATE THEORETICAL VALUE
$1 - \lambda_\beta^2$	−0.0224 (0.021)†	
λ_β^2	1.022	1.06
n_β	0.857 (0.030)†	0.987
τ_o	1.079 (1.12)†	–
τ_{cs}	21.442 (0.89)†	–
c_1	−0.0752 (0.034)†	–
c_2	−0.0214 (0.020)†	–
c_3	−1.329 (0.083)†	–
c_4	−0.4579 (0.022)†	–
$k_o + a_o s/8\mu$	0.0692 (0.012)†	–
k_c	0.1629 (0.038)†	–
k_s	−0.1901 (0.055)†	–
ψ_{BIAS}	0.392 (0.036)†	–

† Estimated 1 σ error bound.

Figure 1 Time-domain reconstructions for original model.

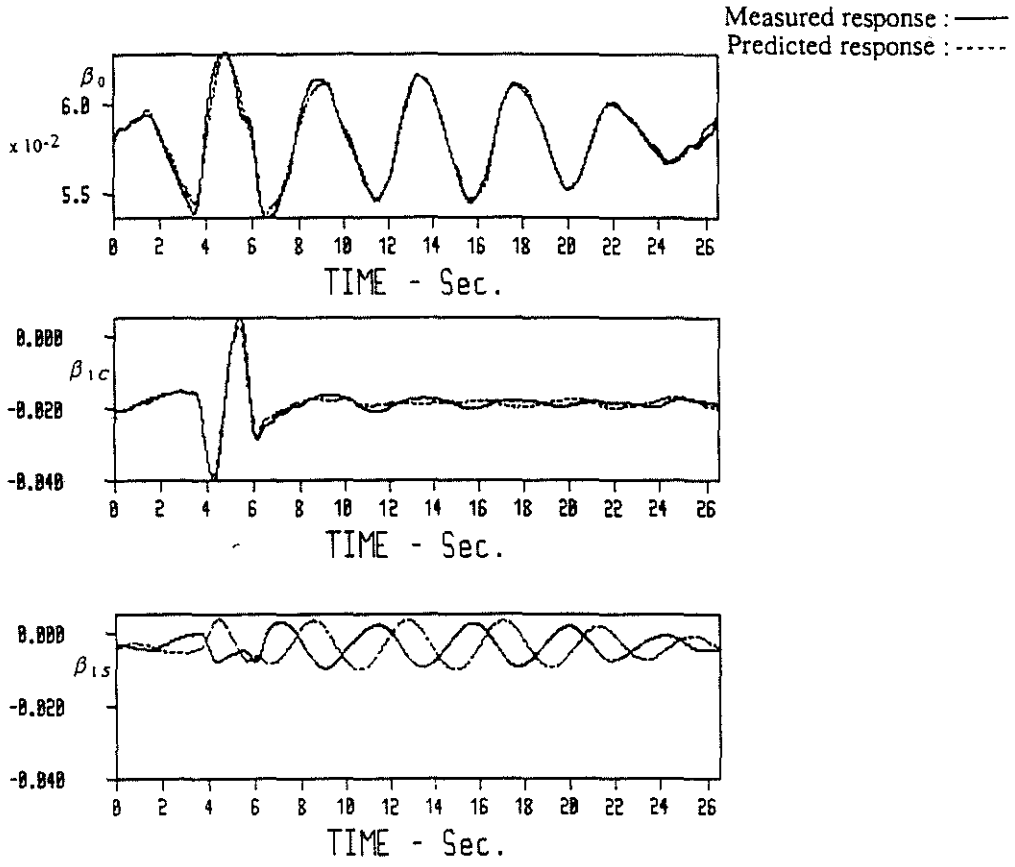

Figure 2 Frequency-domain fits for empirical model.

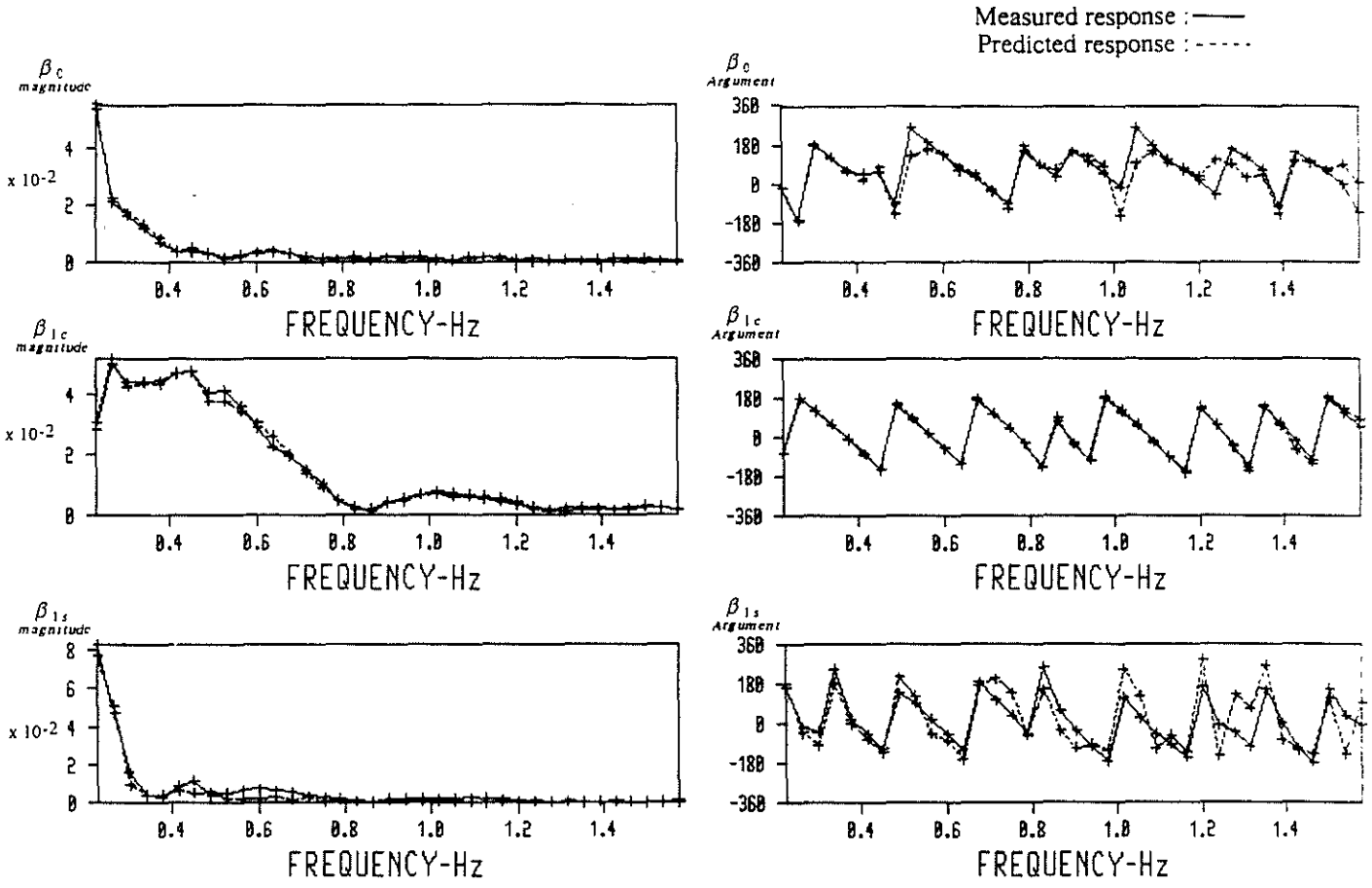

Figure 3 Time-domain reconstructions for empirical model.

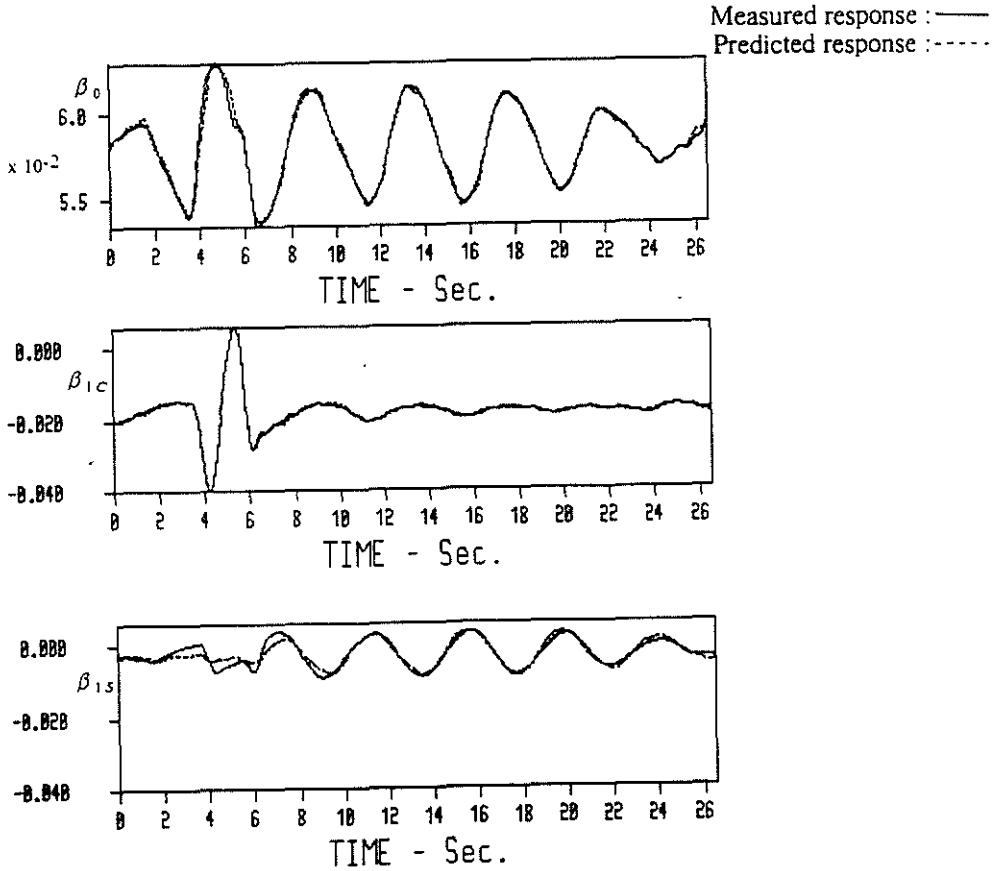

Figure 4 Frequency-domain fits for modified model.

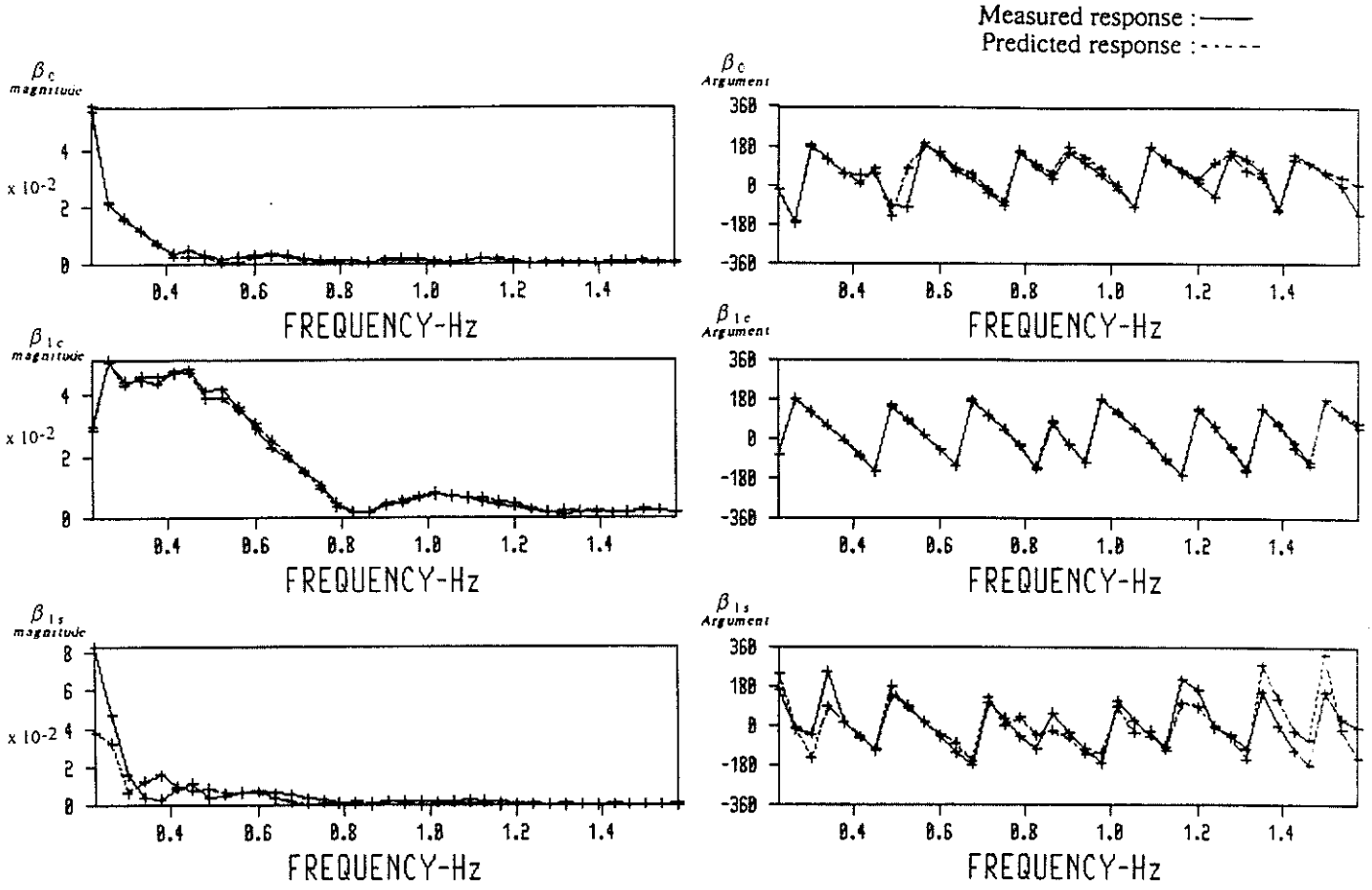

Figure 5 Time-domain reconstructions for modified model.

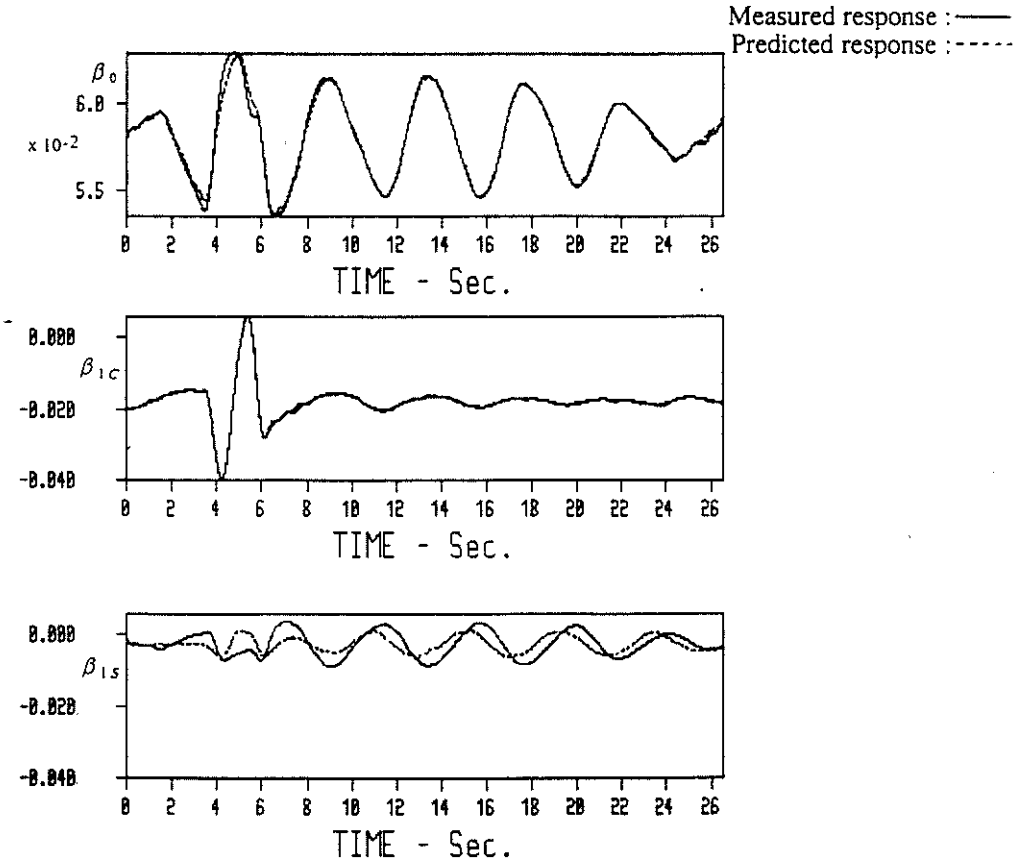

Figure 6 Variation of parameter estimates with lower frequency limit for modified model. Upper frequency limit fixed at 1.58 Hz.